

In-situ Evaluation for Crack Generation Behavior of Iron Ore Agglomeration during Low Temperature Reduction by Applying Acoustic Emission Method and Analysis of Reduction Disintegration Behavior

Moritoshi MIZUTANI*
Takashi ORIMOTO
Tsunehisa NISHIMURA
Kenichi HIGUCHI

Abstract

Iron ore agglomerates such as sinter and pellet are the main raw materials of blast furnaces. Crack generation in their particles during reduction causes the generation of powder and degradation of blast furnace productivity. The objective of this paper is the development of an in-situ evaluation for crack generation and propagation by applying the Acoustic Emission (AE) method. It is possible to analyze the influence of the properties of iron ore agglomerates and reduce gas composition on the crack generation behavior in each stage of reduction and cooling. This method is actually applied to analyses of the properties of iron ore sinter.

1. Introduction

Blast furnaces are countercurrent moving bed reactors of solid particles and gas. The blast volume is closely related to the productivity. To increase and stabilize the blast volume in blast furnaces, the permeability of the gas in the furnaces needs to be improved. **Figure 1** illustrates the relation between the blast furnace permeability and characteristics of iron ore agglomerates. The blast furnace permeability depends on the two factors of the lumpy zone in the upper section and the cohesive zone in the lower section. Charging materials, such as iron ore sinter, pellet, lump, and coke, pulverized due to impact during transportation and as a result of strength decrease due to the reaction in the furnace, deteriorate the permeability of the lumpy zone. Example cases of the latter are reduction disintegration of sinter in the upper section of the furnace at around 550°C, decrepitation of lump ore around 750°C, and hot disintegration of coke that becomes obvious at 1200°C or higher.

Decrease in the strength of iron ore sinter and increase in the reduction disintegration index (RDI) decrease the charging material size and voids in packed beds in the furnace, which increases the gas flow resistance.^{1,2)} In addition, previous study has shown that increase in the quantity of particles 0.5 mm or smaller enhances the gas flow resistance, which increases the buoyancy due to the gas

flow, which causes unstable operation such as hanging of charging materials and gas chaneling.³⁾ Generally, to stabilize the operation of blast furnaces, the blast volume needs to be reduced before such unstable operation occurs. Therefore, increase in the quantity of disintegrated particles in the furnace due to increased RDI deteriorates the productivity.

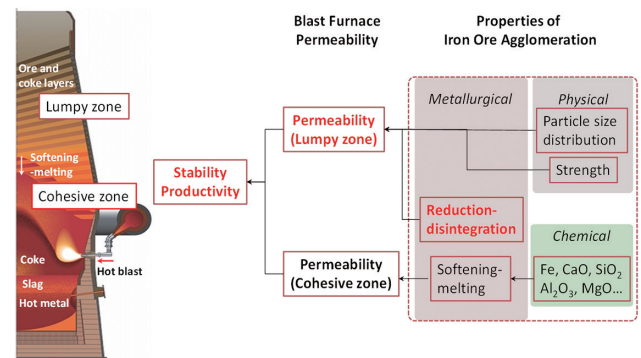


Fig. 1 Relation between iron ore agglomeration and blast furnace permeability

* Researcher, PhD, Ironmaking Research Lab., Process Research Laboratories 20-1 Shintomi, Futtsu City, Chiba Pref. 293-8511

Reduction disintegration is a phenomenon where when iron ore agglomerates, such as iron ore sinter and pellet, and lump are reduced from hematite to magnetite, cracks are formed in the particles and they pulverize in the blast furnaces.⁴⁻¹²⁾ JIS and ISO standards specify using the RDI as an operation management index in off-line tests to evaluate reduction disintegration behavior. The index is obtained as follows: Samples are reduced at a constant temperature with constant gas compositions (e.g., 550°C, 30%CO-70%N₂); the samples cooled to room temperature are subjected to a cold strength test; and then they are sieved. The mass ratio of 3.15-mm or smaller particles to the total mass is RDI. **Figure 2** shows the differences in the reduction disintegration behavior between an actual blast furnace and off-line test. In the off-line test, in addition to reaction degradation due to reduction reaction, cracks may be formed due to thermal stress in the cooling process that is not provided in actual furnaces and thereby the disintegration behavior in the off-line test may deviate from that in the actual furnace. A previous study has shown that changing cooling conditions for reduced samples affects the disintegration behavior; the faster the cooling rate, the higher the disintegrated volume.⁹⁾

From the aforementioned perspective, several test procedures to apply an impact or load during hot reduction have been proposed.¹³⁻¹⁵⁾ However, none of such procedures can evaluate during which of reduction and cooling cracks are formed. As other procedures, *in-situ* observation technologies to monitor iron oxide reduction and crack formation behavior using synchrotron X-ray CT images and laser microscopes have been proposed.^{16, 17)} However, it is difficult for the former to observe 100- μ m or smaller pores and cracks and the latter cannot evaluate cracks inside the samples.

Recently, the acoustic emission (AE) method has been used to analyze cracks and defects in raw materials on a laboratory scale.¹⁸⁻²⁵⁾ The AE method is a non-destructive inspection technology that can detect crack formation and defects in real-time. It is widely used as an equipment testing technology mainly to monitor crack formation in gas holders and other types of structures. However, there have been no reports on the application of the AE method to observe crack formation on iron ore agglomerates such as iron ore sinter and pellets. Therefore, we used the AE method to analyze and evaluate crack formation behavior during reduction. In addition, an *in-situ* evaluation technique for reduction disintegration behavior is proposed based on acquired knowledge.

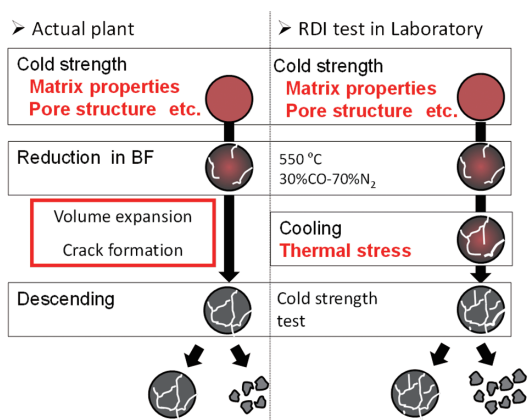


Fig. 2 Factors related to the reduction disintegration phenomenon and different behaviors between actual and off-line test (RDI) conditions

2. Experimental Procedures

2.1 Testing apparatus

Figure 3 illustrates the testing apparatus. This testing apparatus has an AE sensor, an AE measurement system, and a PC for analysis, in addition to a general reduction electric furnace. The AE sensor is VS150-RIC made by Vallen Systeme GmbH and the measurement system is its AMSY-6.^{23, 24)} Generally, an AE sensor needs to be in direct contact with a measuring target.²¹⁾ However, the Curie temperature of the piezoelectric element (e.g., lead zirconate titanate (PZT)) in the sensor is approximately 350°C. At temperatures higher than the Curie point, sensors lose their function, so direct measurement at high temperatures like inside blast furnaces is impossible. Therefore, an indirect measurement method in which a waveguide that transmitted AEs generated in the furnace was adopted.²²⁾ Installing a waveguide (with a diameter of 8 mm and a length of 1000 mm) at the installation location of samples, the reduction disintegration behavior of which is to be evaluated, enables detecting AEs from the samples during reduction continuously. Waveguides proposed in the past were made from resin or alumina. In this test, alumina (made by Techno Ceram Co., Ltd., purity of 99.7%) was used as it had been used at high temperatures of 800°C or higher.

2.2 AE wave analysis procedures

AEs are elastic waves generated when a crack occurs and propagates. **Figure 4a)** shows the AE waveforms detected with an AE sensor. As a definition of AE, the amplitude threshold was set to 40 dB (77.5 V), the rearm time was set to 400 μ s, and the discrete time was set to 200 μ s. The frequency spectrum shown in **Fig. 4b)** was acquired by fast Fourier transform (FFT). The window function and averaging method were adopted with hamming and root mean square (RMS), respectively. Characteristic AE parameters such as the number of counts C, duration time *td*, an amplitude A, AE energy E, and the center of gravity (CoG) of frequency F were recorded by the AE measurement system. A previous study has shown that the amplitude and energy of AEs are correlated with the area of cracks and that the CoG of frequency of AEs varies depending on the material on which cracks are formed and crack types (tensile crack and shear crack).¹⁹⁾

2.3 Samples and experimental conditions

To measure AEs generated during reduction, iron oxide agglomerate reduction in accordance with test procedures, e.g., in ISO 4696-2, was combined with AE measurement in this experiment. As

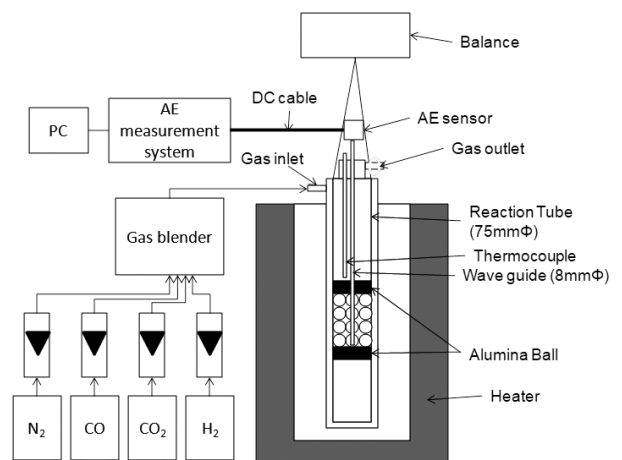


Fig. 3 Schematic of the apparatus used for the reduction experiments with AE measurement system

samples, iron ore sinter, pellets, and lump, the compositions of which are as shown in **Table 1**, were sieved to be grain sizes ranging between 10.0 and 15.0 mm. In this experiment, AE generation behavior during the reduction of packed beds with a total weight of 500 ± 1 g was evaluated. In addition, on the assumption that the contact between a waveguide and samples would affect the detection accuracy of AEs, samples were randomly selected and charged into a reduction furnace such that the bulk density was equal. Specifically, the density of the sintered ore was 1750 kg/m^3 and that of the pellets was 2000 kg/m^3 .

The temperature of the samples was increased to 450, 550, and 650°C in an N_2 atmosphere. The gas was then changed to a $\text{CO-CO}_2\text{-H}_2\text{-N}_2$ mixture to reduce the samples at 15.0 NL/min for 30 minutes. After that, the gas was changed again to N_2 gas and the samples were cooled at 15 NL/min to 373 K. Comparative samples were retained in the N_2 atmosphere for 30 minutes without using the reducing gas and then AEs were measured. The reducibility was calculated based on the gas composition and weight changes during the test.

The samples that had been subjected to the reduction test were then subjected to a rotational strength test at 30 rpm for 30 minutes using a tumbling drum (cylinder with a lifter) with a diameter of 130 mm. Then, each sample was sieved with a 3-mm mesh to measure the weight of samples of 3.0 mm or greater. The RDI was then calculated using Equation (1)

$$\text{RDI} = (1 - W1/W0) \times 100. \quad (1)$$

Where, the RDI is the reduction disintegration index (mass%), $W0$ is the weight of the reduced samples before the rotation test (g), and $W1$ is the weight of the samples remaining on the 3.0-mm mesh (g).

In addition, the reduced samples were cross-sectioned and an optical microscope was used to observe the type, size, and location of cracks qualitatively.

3. Experimental Results and Consideration

3.1 Characteristics and behavior of AEs generated during reduction

Figure 5 shows changes in the AE energy and AE counts measured in the test. The AE counts when the N_2 gas was used for the

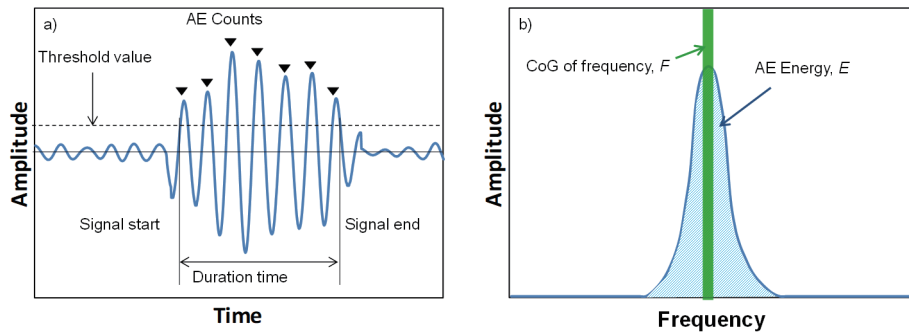


Fig. 4 Examples of AE characteristic parameter in an AE hit: a) AE waveform and b) AE frequency spectrum

Table 1 Chemical compositions of samples

Sample	Total Fe (mass%)	FeO (mass%)	SiO ₂ (mass%)	Al ₂ O ₃ (mass%)	CaO (mass%)	MgO (mass%)	C/S (-)
Sinter A	57.62	8.74	5.41	1.60	10.39	1.01	1.92
Sinter B	58.01	6.08	5.23	1.82	9.36	0.93	1.96
Pellet A	63.88	1.62	6.43	0.38	0.48	0.66	0.07
Pellet B	63.39	0.57	3.45	0.39	1.10	1.15	0.32
Pellet C	65.93	0.66	2.36	0.54	2.62	0.01	1.11

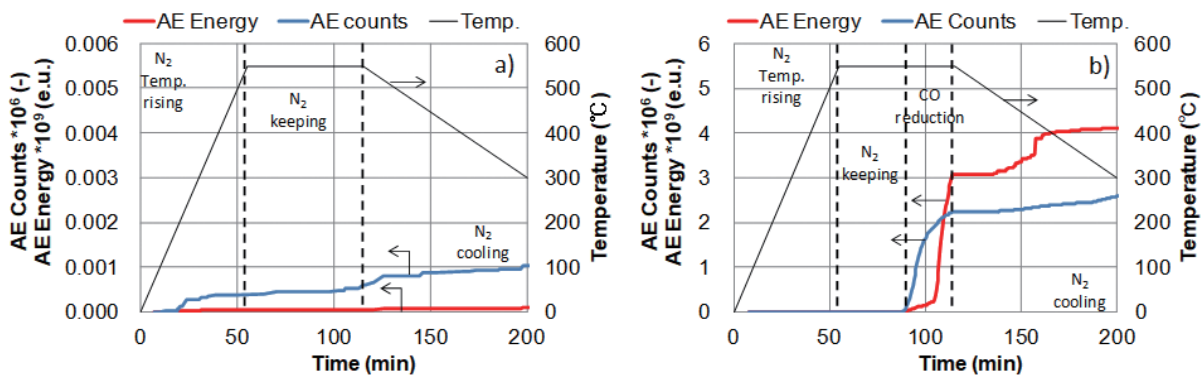


Fig. 5 Trends in AE counts and AE energy during reduction disintegration tests: a) N_2 keeping and b) CO reduction

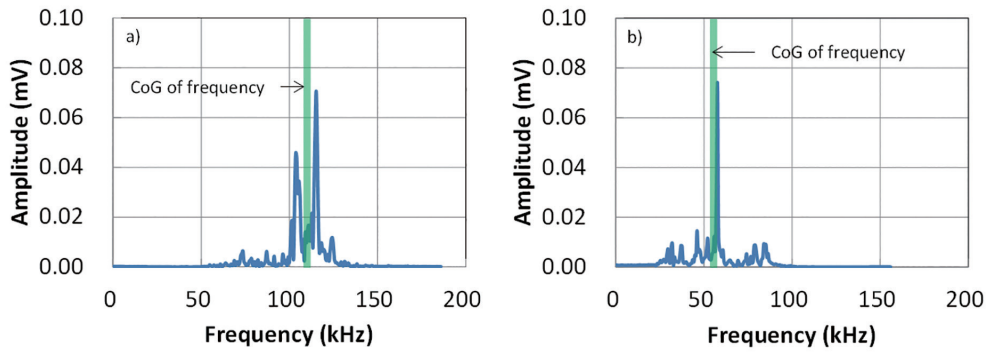


Fig. 6 Examples of AE waveform generated a) during CO reduction and b) during N₂ cooling after reduction

temperature increase were 100 or less and the energy was low. This indicates that noise in the measurement environment was not detected. On the other hand, in the case of CO reduction, the detected AE energy was 100 times or higher than in the N₂ case and a large number of AEs was also detected during cooling unlike in the N₂ case.

Figure 6 shows example AE spectra generated during the reduction and cooling. The frequency of the AEs during the CO reduction was 90 kHz or higher. On the other hand, during the N₂ cooling, specific frequencies equal to or lower than 60 kHz were detected. These results show that the frequency bands of the AEs generated vary between the stages. The different AE frequency bands between the reduction and cooling can be attributed to the difference in the crack generation mode. Otsu et al. classified the fracture mode by using the average frequency and the RA value, which is the ratio of the rise time and the maximum amplitude, and reported that the tensile crack mode is of high frequency and the shear crack mode is of low frequency.¹⁹⁾ This suggests that tensile cracks are generated by volume expansion during reduction and shear cracks are generated by volume shrinkage during cooling.

Figure 7 shows example CoG of frequency of AEs generated during the test. Three types of AEs having frequency bands in the range of (a) 65–95 kHz during the temperature increase, (b) 95 kHz or higher during the reduction, and (c) 65 kHz or lower during the cooling were detected. AEs in the frequency (a) were also detected in the case of N₂ atmosphere, so it was estimated that they were elastic waves caused by the friction between the sample and waveguide due to thermal expansion and thereby they do not contribute to reduction disintegration. AEs in the frequency (b) were not detected in the case of N₂ atmosphere, so they are presumably caused by cracks formed during the reduction. AEs in the frequency (c) may be caused by cracks formed due to thermal stress during the cooling. In addition, in the case of CO reduction, AEs with high energy shown in the warm colors were detected at an early stage of the reduction while in the case of H₂ reduction, AEs with high energy were detected in a later stage of the reduction. This indicates that H₂ reduction causes more cracks than CO reduction.

3.2 Observation of cracks formed during reduction

Figure 8 shows example microstructures of the sintered ore and pellets during the CO and H₂ gas reductions. The “R.D.” in the figure refers to the reduction degree of the samples after the test. Under all the test conditions, the reduced samples had cracks. The iron ore sinter had more linear and larger cracks than the pellets. In addition, although the reduction reaction on the iron ore sinter advanced starting from any location of the samples regardless of the reduction conditions, the H₂ gas reduction tended to cause more cracks than the CO gas reduction. On the other hand, regarding the reduction of

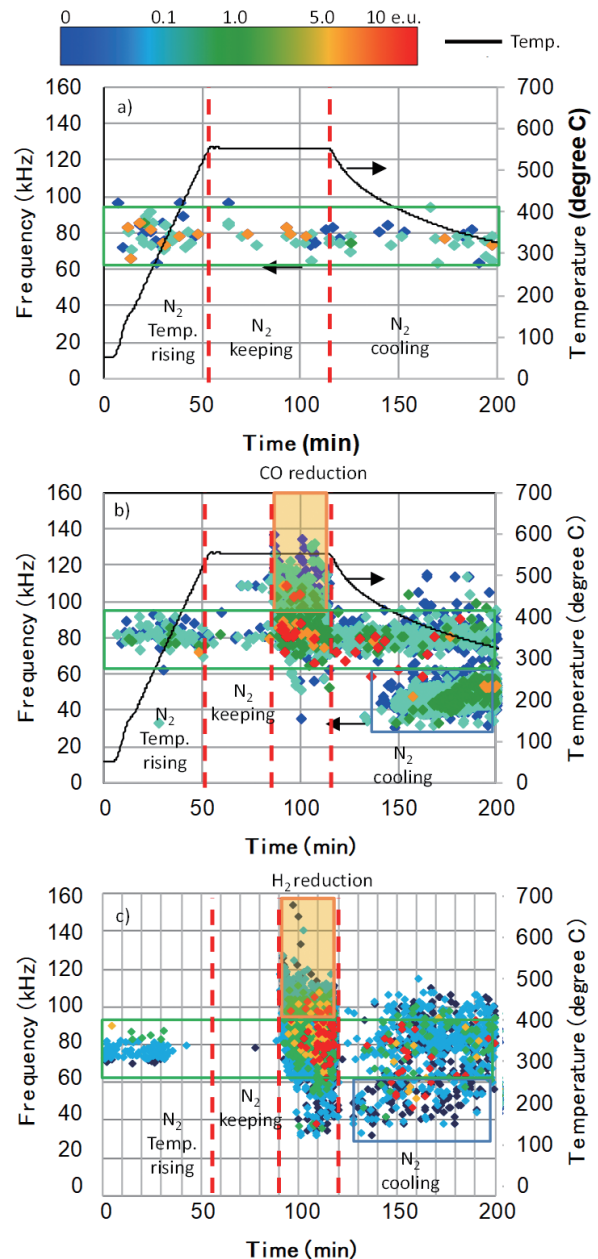


Fig. 7 Examples of CoG of frequency of AE of sinter A a) N₂ keeping, b) During CO reduction, c) During H₂ reduction

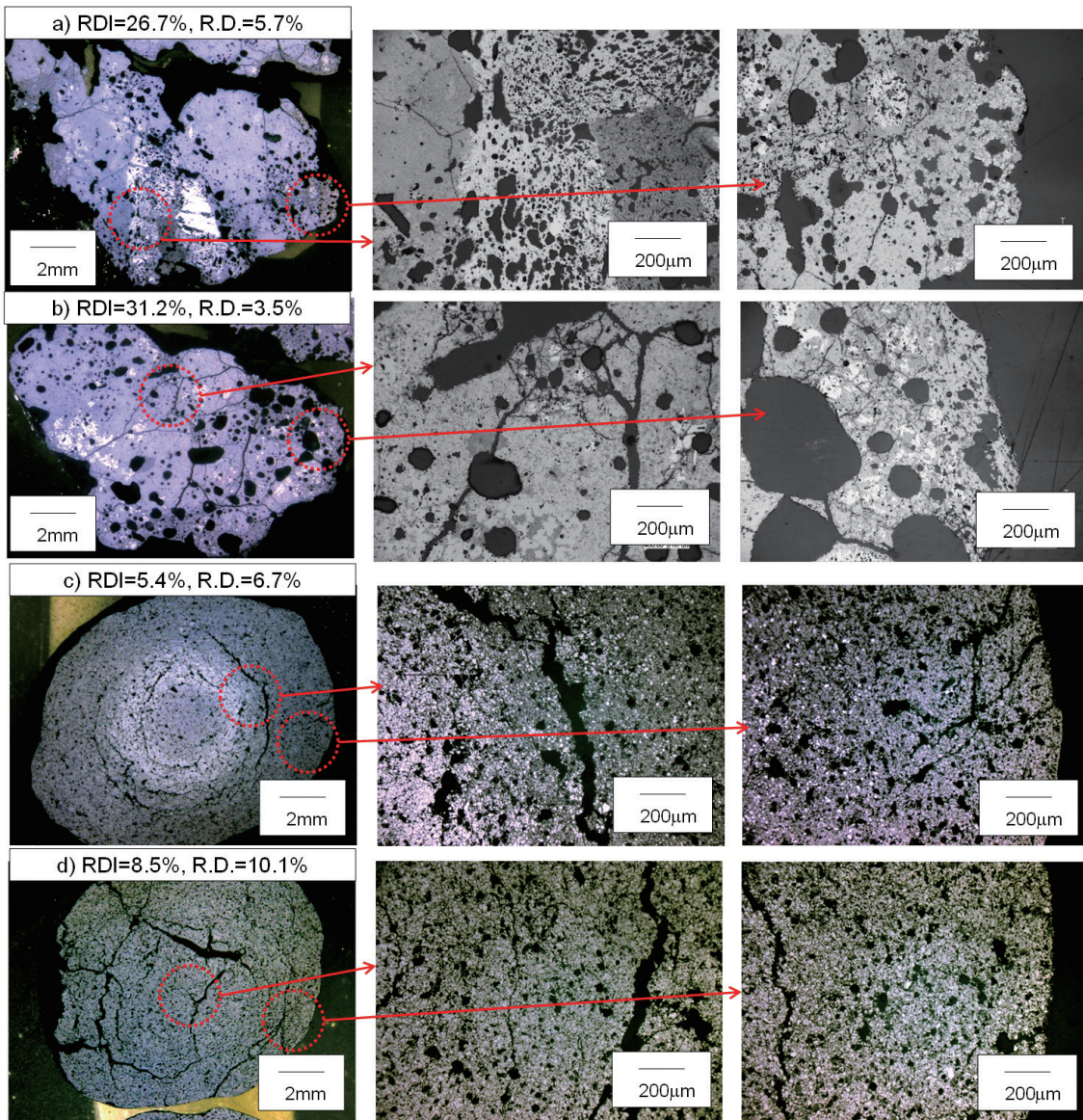


Fig. 8 Microstructure of sinter A and pellet A reduced at 823 K for 1.8 ks
 a) Sinter A, 30%CO-70%N₂, b) Sinter A, 30%H₂-70%N₂, c) Pellet A, 30%CO-70%N₂, d) Pellet A, 30%H₂-70%N₂

the pellets, the reaction pattern and crack formation behavior varied depending on the gas composition. In the case of CO gas reduction, the reduction reaction tended to travel to unreacted nuclei and concentric cracks were formed. On the other hand, the reaction pattern in the H₂ gas reduction tended to even out and many various-sized radial cracks were seen from the surface of the samples to the center. These observation results are consistent with the crack formation behavior assumed from AE generation behavior, which indicates that AE measurement enables analogizing how cracks are formed due to low-temperature reduction reaction.

Figure 9 shows observed silicate slag (SS) and calcium ferrite (CF) phases existing in the iron ore sinter before and after the reduction. These photographs show that the SS and CF phases after the reduction have many cracks while the hematite hardly has any cracks. These results show that cracks may have formed on the surrounding SS and CF phases due to volume expansion during the reduction from the hematite to magnetite. When focusing on the shape

and quantity of cracks, many linear cracks are seen on the SS phase, while arc-shaped cracks are seen on the CF phase although the quantities are small.

3.3 Relation between AE energy and reduction disintegration behavior

In the AE measurement test during the reduction of the packed beds in this study, it is difficult to separate AEs generated by the friction that correspond to noise from AEs generated when sintered ore and pellets are reduced completely, for evaluation. Therefore, AEs were simply classified based on the frequency as shown below. First, 65–95 kHz (1) was excluded from the analysis target as it derived from the friction between samples and waveguide; and (2) AEs that may be attributed to the reaction deterioration during the reduction were separated from (3) AEs derived from the thermal stress during the cooling, both of which may have derived from crack formation that would affect reduction disintegration. Figure 10 shows the relation between the total AE energy of (2) and (3) and

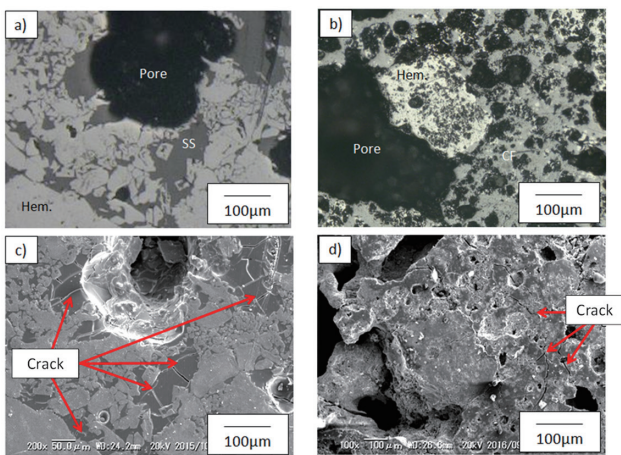


Fig. 9 Surface texture of iron ore sinter before and after reduction
 a) Hematite + SS before reduction, b) Hematite + CF before reduction, c) Hematite + SS after reduction, d) Hematite + CF after reduction

the RDI. The figure shows that the aforementioned simple treatment is sufficient to evaluate the reduction disintegration behavior by the AE method since the AE energy is collative with the RDI.

Figure 11 shows the relation of the AE energy between (2) AEs that may be attributed to the reaction deterioration during the reduction and (3) AEs derived from the thermal stress during the cooling. AEs (3) are generated during the cooling that is a process specific to laboratory tests and thereby it is presumed that they do not relate to disintegration in actual furnaces. However, their energy is higher than that of (2) that is assumed to correspond to disintegration in actual furnaces. Particularly, the contribution of (3) is higher in the case of iron ore sinter than that in the case of pellets. These results suggest that the conventional RDI, which determines the strength of reduced sintered ore after cooling, cannot evaluate its reduction disintegration behavior in actual furnaces accurately.

4. Conclusion

Nippon Steel Corporation developed the *in-situ* evaluation apparatus that can evaluate low-temperature reduction disintegration in reduction tests in combination with the AE method. The apparatus was used to measure AEs generated when iron oxide agglomerates were reduced at low temperatures to study the formation and propagation behavior of cracks. Using alumina waveguides can detect AEs generated during reduction indirectly and accurately. A large quantity of AEs is generated during cooling besides during reduction. Therefore, the conventional reduction disintegration evaluation index RDI cannot express the reduction disintegration behavior in actual furnaces without a cooling process accurately.

In addition, the influence of the properties of iron ore agglomerates and reduction gas conditions on reduction disintegration behavior at low temperatures could be recognized thanks to the frequency and energy of AEs analyzed based on the measured AE waveforms. Comparing to iron oxide pellets of which the main constituent mineral phase is hematite, many cracks were formed on calcium ferrite and silicate slag in the case of the iron ore sinter and the frequency of the AEs generated during the reduction tended to be low. In addition, the test has confirmed that the RDI correlates with the total AE energy derived from the volume expansion during the reduction and thermal stress during the cooling and that the quantity of cracks formed during the H₂ gas reduction where reaction patterns tend to develop evenly is large.

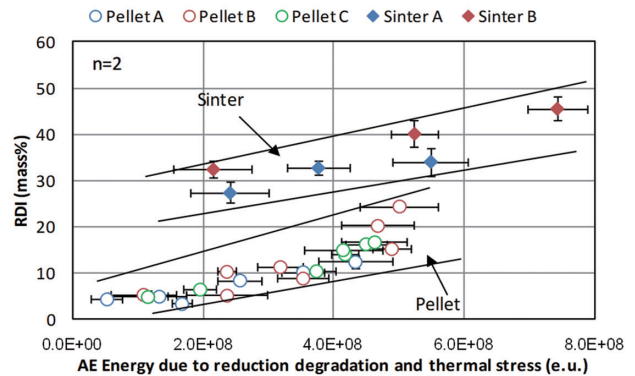


Fig. 10 Relation between the AE energy and reduction disintegration index (RDI)

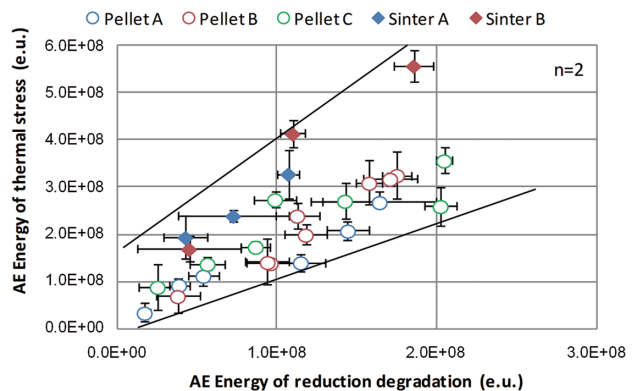


Fig. 11 Relation between the AE energy of reduction degradation and thermal stress

Acknowledgments

We express our deep gratitude to Professor Eiki Kasai at the Graduate School of Environmental Studies, Tohoku University for his exceptional guidance. We also express our appreciation to Mr. Daisuke Kudo and other members of the process testing team, Nippon Steel Technology Co., Ltd. for their support to our experiment.

References

- 1) Nogami, H. et al.: Tetsu-to-Hagané. 100, 119 (2014)
- 2) Lu, L. et al.: Quality Requirements of Iron Ore for Production. Iron Ore. 1st Ed. Cambridge, Woodhead Publishing, 2015, 482p
- 3) Sasaki, M. et al.: Tetsu-to-Hagané. 68, 563 (1982)
- 4) Sawamoto, N. et al.: Tetsu-to-Hagané. 70, 512 (1984)
- 5) Inazumi, T. et al.: Tetsu-to-Hagané. 68, 2207 (1982)
- 6) Shigaki, I. et al.: Tetsu-to-Hagané. 68, 1513 (1982)
- 7) Taguchi, N. et al.: Tetsu-to-Hagané. 69, 1409 (1983)
- 8) Haruna, J. et al.: Tetsu-to-Hagané. 69, S742 (1983)
- 9) Iwanaga, Y. et al.: Tetsu-to-Hagané. 77, 2115 (1991)
- 10) Murakami, T. et al.: ISIJ Int. 52, 1447 (2012)
- 11) Murakami, T. et al.: ISIJ Int. 55, 1181 (2015)
- 12) Murakami, T. et al.: ISIJ Int. 55, 1197 (2015)
- 13) Linder, R.: JISI. 189, 233 (1958)
- 14) Jomoto, Y. et al.: Tetsu-to-Hagané. 57, 1606 (1971)
- 15) Machida, S. et al.: CAMP-ISIJ. 26, 201 (2013)
- 16) Kim, J. R. et al.: ISSTech 2003 Conference. p. 175
- 17) Kashiwaya, Y. et al.: ISIJ Int. 47, 226 (2007)
- 18) Enoki, M. et al.: Journal of the Japan Institute of Metals. 58, 418 (1994)
- 19) Ohtsu, M.: Research in Nondestructive Evaluation. 6, 169 (1995)
- 20) Ito, K. et al.: Materials Transactions. 53, 671 (2012)
- 21) Nakamura, H.: Journal of The Japanese Society for Non-Destructive Inspection. 62, 267 (2013)

- 22) Briche, G. et al.: Journal of the European Ceramic Society. 28, 2835
(2008)
23) Nakamura, H.: IIC REVIEW. 56, 28 (2016)
24) Nakamura, H.: IIC REVIEW. 57, 3 (2016)
25) Farnam, Y. et al.: Cement and Concrete Composites. 60, 135 (2015)



Moritoshi MIZUTANI
Researcher, PhD
Ironmaking Research Lab.
Process Research Laboratories
20-1 Shintomi, Futtsu City, Chiba Pref. 293-8511



Takashi ORIMOTO
Chief Researcher
Ironmaking Research Lab.
Process Research Laboratories



Tsunehisa NISHIMURA
Senior Researcher, Dr. Eng.
Ironmaking Research Lab.
Process Research Laboratories



Kenichi HIGUCHI
Chief Researcher, Dr. Eng.
Ironmaking Research Lab.
Process Research Laboratories